Open Ceramics 16 (2023) 100448

Contents lists available at ScienceDirect

Open Ceramics

journal homepage: www.sciencedirect.com/journal/open-ceramics

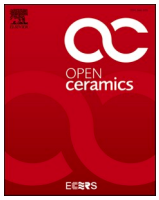

Impact of the reduction of graphite content in critical properties of MgO–C bricks for steelmaking industry

M.N. Moliné [a], S.E. Gass [a,*], P.G. Galliano [b], D. Gutiérrez-Campos [c], A.G. Tomba Martinez [a]

[a] Instituto de Investigaciones en Ciencia y Tecnología de Materiales (INTEMA), CONICET – Facultad Ingeniería / UNMdP, Av. Colón 10850, 7600, Mar del Plata, Argentina
[b] Tenaris Siderca, Dr. Simini 250, 2804, Campana, Argentina
[c] Departamento de Ciencia de los Materiales, Universidad Simón Bolívar, Edificio MEM, Piso 2, Valle de Sartenejas, Baruta, Edo. Miranda, Apartado Postal 89000, Caracas, 1080, Venezuela

ARTICLE INFO

Handling Editor: Dr P Colombo

Keywords:
MgO-C refractories
CO_2 emissions
Mechanical properties
Oxidation resistance

ABSTRACT

Nowadays, the use of lower amounts of graphite in MgO–C bricks for the steelmaking industry is motivated by several reasons, including the reduction of CO_2 emissions. In this work, a MgO–C brick with 12 wt% graphite, was evaluated in comparison with a similar material containing just 8 wt% of this component. The changes induced in the brick by thermal treatments (graphite bed) between 500 and 1400 °C were analyzed comparatively. Moreover, the effect of reducing the graphite content in the mechanical properties at RT, 1000 and 1400 °C (compressive tests, in argon) and the oxidation resistance in air at 1000 and 1400 °C was determined. At 1000 °C, the refractory with 8 wt% graphite exhibited the highest mechanical strength and stiffness. Furthermore, although the decarburized area was larger after treatment at 1000 °C in air in this brick, the mass and carbon losses showed the opposite trend.

1. Introduction

Most industrial processes generate harmful effects such as CO_2 emissions, whose control needs to be improved to reduce environmental pollution. Primary economic sectors, like steelmaking, are responsible for contributing with huge amounts of CO_2 from high-temperature processes. In this regard, intelligent refractory solutions in steel production will reduce specific energy and CO_2 emissions [1,2]. MgO–C refractory bricks are used on a large scale in this industry, being at the top of the ranking of materials for steelmaking, and they contribute to the overall CO_2 emissions of steel manufacture, mainly due to the carbon content (as both graphite and pyrolytic carbon are used) [3,4]. Since the 1980′s MgO–C composites have been developed and, nowadays, the steel industry employs refractory linings built up with products having typically 10–20 wt% of graphite flakes [5,6], depending on the specific conditions of the operation, in order to guarantee a good performance of the vessel (ladle, BOF, EAF, etc.) and high efficiency of the process. However, to meet the requirements of clean steel production and low energy loss, the amount of graphite in the refractories' composition are tending to be reduced toward the use of 'low carbon MgO–C bricks' [6–8]. When carbon content is reduced in MgO–C materials, thermal and thermochemical properties are affected such as thermal spalling and corrosion resistance at high temperatures. On the other hand, a greater carbon percentage leads to increased carbon pick-up by steel, higher heat losses, and more CO and CO_2 gas by-products are generated. Thus, low-carbon MgO–C bricks with desired properties are currently widely studied in order to keep maximum productivity in steelmaking and to reduce the carbon footprint, which should motivate any actions in this direction.

Since it is not an easy task to counterbalance the impact of reducing the carbon content in the MgO–C bricks with the requirements in service of refractory linings during clean steelmaking, there are still a great number of studies devoted to deep knowledge about the diminishing of graphite content in MgO–C bricks and its effects on the final properties of the refractory materials. Thus, over the last decade, several works have evaluated the effects of lowering the graphite amount in the brick's composition on its main properties [5,6,9–13] and others have proposed different routes to reduce the negative impacts by using alternative raw materials [14–25]. Even though some studies were successfully explored at a laboratory scale and promising results were obtained [13,17,26], these new developments have not yet been transferred to industrial practice, in most cases.

* Corresponding author.
E-mail address: segass@fi.mdp.edu.ar (S.E. Gass).

https://doi.org/10.1016/j.oceram.2023.100448
Received 14 July 2023; Received in revised form 28 August 2023; Accepted 29 August 2023
Available online 1 September 2023

Another important issue related to MgO–C materials is the organic binders used to manufacture refractory products without ceramic bonds; these binders have evolved from a traditional pitch to different phenolic resins. In the last decades, a new generation of binder systems have been incorporated, which have even better carbon yield and oxidation resistance, together with lower or even zero BaP emissions [13,26–31]. These eco-friendly binders have mitigated environmental and health complex problems when compared to other carbonaceous binders. Furthermore, the residual carbon from the binder pyrolysis has an influence on several of the physicochemical properties of MgO–C bricks; the oxidation resistance, for instance, is rather affected by the quality of the carbonaceous structure formed at the end of the pyrolysis. Compared to the sole phenolic resin, it has been reported that its mixing with an eco-friendly binder, based on a chemically modified pitch, increased the oxidation resistance by a significant degree, especially at temperatures higher than 1000 °C [32].

The present work, being part of the research project of our lab group, focuses the analysis on the effect of reducing the graphite content on the mechanical and chemical properties at high temperatures (1000 and 1400 °C) of MgO–C refractories. A brick with 12 wt% of graphite, a typical content for the steelmaking industry, is used as a reference, and the results are compared with a similar refractory composition having just 8 wt% of graphite. Moreover, aligned with the aim of reducing the environmental impact, a combination of a phenolic resin with an eco-friendly binder was employed in the bricks' formulation. In order to obtain a profound understanding of the behavior between the two studied refractories (8 and 12 wt% of graphite), the thermal evolution of the materials was also analyzed between 500 and 1400 °C.

2. Materials and methods

Two MgO–C refractory bricks, based on fused and sintered magnesia particles (70/30 mass ratio), and 3 wt% of a binder system, were specially manufactured in-plant using the current industrial processes for commercial products. The binder (soft-bonding system, SB) is a combination of a resol resin (thermal curing) and a chemically modified pitch powder (CarboRes® [32]). Two contents of graphite flakes were evaluated: 12 wt% (SB12-0 brick) and 8 wt% (SB8-0 brick). After pressing, the bricks were tempered/cured at ~300 °C (the complete thermal treatment lasted ~8 h) to cure and stabilize the binder system. Characterization of the as-received MgO–C bricks was conducted using a vast group of analytical techniques that were described and referenced elsewhere [33] as part of our research line; the main data are summarized in Table 1. Also, from the porosimetry data, just the distribution of pores smaller than 13 μm was also obtained (in order to be compared with the pore-size distribution of the thermal-treated samples) and this pore-sizes profile is shown in Fig. 1 for SB12-0 and SB8-0.

Granulometric differences observed between SB12-0 and SB8-0 (see Table 1) indicate that a granulometric profile was introduced to achieve similar global densities for both bricks and suggest that the addition of a higher percentage of graphite was done at the expense of the finer magnesia particles [33]. A lower proportion of graphite in the bricks' composition reduced the porosity, the mean size of pores, and the permeability of the structure. When the graphite content change from 12 to 8 wt%, the distribution of pore sizes showed a significant increase of smaller fractions, i.e., pore sizes below 15 μm. It can be seen in Table 1 that 83.4 vol% of pores in SB12-0 are larger than 15 μm while only 21.4 vol% of pores in SB8-0 are in this range (>15 μm). Moreover, from the same porosimetry evaluation of the as-received MgO–C bricks [33], it was determined that the volume of pores <1 μm increased from ~10 vol % for SB12-0 to ~30 vol% for SB8-0; these considerations about pore-size profile are meaningful since it has been reported the importance of small voids for resisting fluids penetration [34].

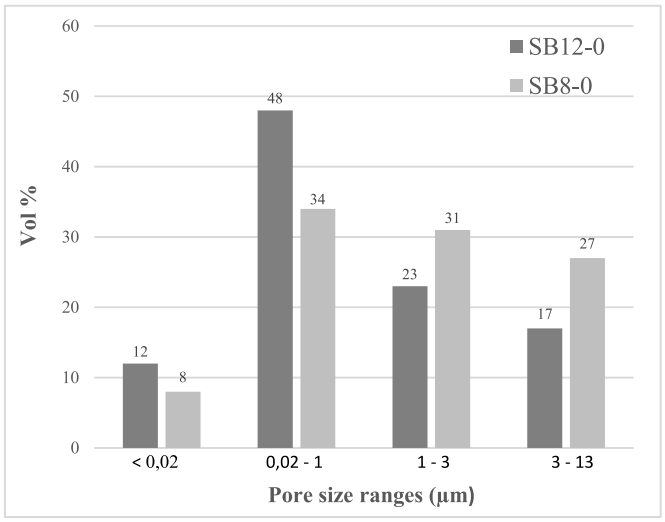

Fig. 1. Pore-sizes distribution for pores <13 μm of the as-received MgO bricks.

Table 1
Characteristics of the as-received MgO–C bricks.

		SB12-0	SB8-0
Pycnometric density (g/cm^3)		3.16 ± 0.06	3.24 ± 0.04
Bulk density (g/cm^3)		2.94 ± 0.05	3.05 ± 0.05
Apparent porosity (%)		4.1 ± 0.6	3.4 ± 0.6
Closed porosity (%)		~2.2	~2.4
Permeability (cm^3/dyn/s)		~1.4	~1.0
Pore sizes (vol%)	<0.02 μm	1.7	6.3
	0.02–3 μm	11.4	50.3
	3–15 μm	3.5	22.1
	>15 μm	83.4	21.3
Particle sizes (wt.%)	≥7200 μm	1.0	0.0
	<1190 μm	65.2	64.3
Carbon content (wt.%)[(1)]		13.0 ± 0.1	10.2 ± 0.1
Maximum mass loss (wt.%)[(2)]		14.7	11.6

[1] Determined by C LECO technique.
[2] Estimated by TGA in air.

In order to appraise the impact of the reduction of graphite content in critical properties of MgO–C materials, three sets of cylindrical specimens (25–30 mm in diameter and 25–40 mm in height) of both refractory compositions (SB12-0 and SB8-0) were thermally treated in a graphite bed at different conditions: (1) 5 h at 500 °C, (2) 1 h at 1000 °C and (3) 1 h at 1400 °C. An electric furnace (house-constructed) was employed for each treatment, with a heating and cooling rate of 5 °C/min. Thermally treated samples were characterized by bulk density and apparent porosity measurements according to DIN EN 993-1 [35]. In all cases, kerosene at 37 °C was the reference liquid and a Sartorius BP 221 S balance was used. In addition, the carbon content was determined by the C LECO technique (CR12 LECO equipment) on powder samples (<1 mm) or estimated from TGA curves (in air) of the thermally treated materials. The pore size distribution was determined in the range of 0.0734–13 μm (mesopores) by mercury intrusion porosimetry using a Pascal 440 Thermo Scientific instrument on ~0.6 cm^3 samples.

The mechanical behavior of the as-received MgO–C refractories was evaluated at room temperature (RT), 1000 and 1400 °C by applying a compressive load to obtain stress-strain (s-s) curves, using an internal protocol [36]. A testing machine Instron model 8501 was used setting a displacement rate of 0.1 mm/min up to the specimen's failure. An Instron capacitive extensometer (±0.6 μm) suitable for room and high temperatures was employed to measure the axial displacement of the cylindrical specimens (30 mm in diameter and 45 mm in height). Tests were carried out, at least, in duplicate. An electric furnace (Termolab, Fornos Eléctricos Lda) was coupled to the framework for high-temperature testing. An argon flow (purity: 99.995%) at 5 L/min was introduced into a ceramic chamber to keep an inert atmosphere surrounding the specimen. During heating, a slight pre-load was applied

to maintain the contact between the specimen and the load-bearing system. Before the application of the increasingly compressive load, the specimen was maintained at the testing temperature for 30 min. Mechanical parameters were determined from the s-s curves: (1) fracture strength (σ_F), corresponding to the stress value for the maximum load, (2) fracture strain (ε_F), which is the strain corresponding to the maximum load and (3) secant modulus ($E_{0.001}$), calculated as the slope of a secant line to the s-s curve from the origin to 0.001 of deformation.

An estimation of the mass lost by the samples during the compressive mechanical testing at high temperatures was conducted using the TGA thermograms (in air) of the as-received bricks and the mechanically tested specimens, both as powdered samples. The delta between the maximum mass losses (which take place at ~1000 °C) in the thermograms of the as-received brick and the mechanically-tested specimen was considered as the mass lost during the mechanical test, and designated as Δm_m (%).

The refractory's sensitivity to an oxidant atmosphere (air) was analyzed in duplicate, via the isothermal treatment of cylindrical specimens (25 mm in diameter and 25 mm in length) in an air environment (0.21 atm of O_2) at 1000 and 1400 °C. An electric chamber furnace (house-constructed) was used with the following heating schedule: heating at 5 °C/min until the testing temperature, holding the testing temperature for 1 h, and then, cooling the samples at 5 °C/min till room temperature. The specimens tested at 1000 °C were previously treated at 500 °C for 5 h in a graphite bed and just the lateral area of the cylinders were in contact with the surrounding air. In the case of samples tested at 1400 °C, the flat top surface of the cylinders was also exposed to the furnace atmosphere. Then, the tested cylinders were vacuum-packed in polyester resin and cut crosswise. The mass loss, named as Δm_O, and the decarburized superficial area, both in percentages, were estimated as oxidation degree indicators. Images of both cross surfaces of each sample were analyzed using Image-Pro Plus v.6 software to appraise the decarburized area, which was considered as the peripheral region in which a reduction of the black or dark color was visually detected. A radius delimiting the decarburized region from the central darker zone was defined, from which the decarburized area was calculated. The percentage of the total cross-section corresponding to the decarburized area of the specimen was considered as the oxidation indicator.

3. Results and discussion

3.1. Material evolution during thermal treatments (graphite bed)

During a thermal treatment at 500 °C, the main process taking place is the organic binder pyrolysis; it is accompanied by volatile compounds elimination that produces mass loss and the formation of channels for gases escape. When the temperature of the treatment increases to 1000 °C, some processes, that could begin at a lower temperature, advance: the volatile elimination and the formation of a condensed C–C structure, the 'residual carbon', due to the binder pyrolysis -this last process accompanied by volume contraction- and the oxidation of the different sources of carbon (the residual carbon first, and then, the graphite). Even the thermal treatments have been performed in graphite bed to minimize the occurrence of this last process it cannot be complete discarded [26,32,37]. At 1400 °C, the carbothermal reduction of MgO could also take place in the MgO–C bricks, which involves the generation of gases such as CO and Mg; however, the oxidation of $Mg_{(g)}$ when it comes in contact with $O_{2(g)}$ at the specimen external surface may produce the crystallization of MgO in the structure voids. Such processes are responsible for the changes in the textural characteristics and the composition of SB12-0 and SB8-0, reported in Table 2 (T represent the treatment temperature), after thermal treatments in this thermal range (500–1400 °C).

As the temperature of the treatment increased, more amounts of open pores were formed, which was associated to the formation of channels for volatiles escape and the mass loss, being the change more notable between 500 and 1000 °C. In tune, the specimens treated at 500 °C (see Table 2) exhibited higher contribution of small pores (<3 μm) with respect to the original materials (as-received SB12-0 and SB8-0 have ~83 and ~73 vol% of pores <3 μm, respectively, as shown in Fig. 1), but the opposite trend was observed for the treatment at 1400 °C, which was attributed to the coalescence of small voids to form larger pores (due to the volatiles escape and the oxidation of carbon). Meanwhile, the mass loss increased just after the treatment at 1400 °C, as expected.

Table 2
Characteristics of materials after thermal treatments in graphite bed.

	T (°C)	Apparent porosity (%)	Pores volume (vol%)		Carbon content (wt. %)	Mass loss (wt.%)
			<1 μm	<3 μm		
SB12–0	500	5.5	54	88	13.4[1]	1.4
	1000	11.0	59	82	~13.3[2]	1.4
	1400	11.2	54	79	12.8[1]	2.7
SB8-0	500	6.7	28	78	9.9[1]	1.5
	1000	9.3	57	80	~9.4[2]	1.5
	1400	9.6	41	70	9.6[1]	3.0

[1] Determined by C LECO technique.
[2] Estimated from TGA curves of the thermally-treated materials.

Regarding the effect of the reduction in graphite content from 12 to 8 wt% in the open porosity of the materials, it should be noticed that at 500 °C the sample with higher graphite content (SB-12-0) presented a lower percentage of apparent porosity (5.5%) than the material with reduced graphite content (SB-8-0), which showed 6.7% of apparent porosity. Moreover, the contribution of pores <1 μm, which are considered those which resist the fluids penetration, was higher for SB12-0 after the treatment at 500 °C (54 vol%) with respect to 28 vol% of SB8-0, but near to the original brick (60 vol% from Fig. 1). However, when lower amount of graphite was present (SB8-0), the volume percentage of pores smaller than 1 μm showed a significant drop (from the as-received with ~42 to 28 vol% of SB8-0 treated at 500 °C). These changes suggest that the permeability of materials after this thermal treatment increased more when lower amount of graphite was used.

As is shown in Table 2, the content of carbon for SB8-0 after treatment at 500 °C was slightly lower than the original bricks (Table 1), conversely to that observed for SB12-0. Meanwhile, the former exhibited a slightly larger mass loss (1.5 vs 1.4 wt%) during the treatment at 500 °C. This fact, together with the textural changes discussed above was attributed to soot formation ($2\,CO_{(g)} \rightarrow CO_{2(g)} + C_{(s)}$) [37,38]; taken into account the differences in the characteristics of SB12-0 and SB8-0 after the treatment, this type of carbon was produced in a higher degree in SB12-0 than SB8-0.

Conversely to that observed after the thermal treatment at 500 °C, the volume of open pores, when the temperature reached 1000 °C, increased to a lower degree for SB8-0 compared with SB12-0, which exhibited a higher value of apparent porosity, like in the as-received materials (with no thermal treatment). In tune, the proportion of small pores (<3 μm) resulted similar for both materials. In this case, it should be considered that as the pyrolysis of the organic binder advanced to a larger degree under this thermal condition, the characteristics of the graphite flakes and how are they distributed in the refractory structure, will be more determining for the material's texture. According to previous reports, the presence of Mrozowski cracks in graphite particles favors the separation of sheets in the flake at temperatures around 1000 °C [39,40], contributing to the porosity increase; a greater effect is expected for a higher amount of graphite, and these facts could explain the differences in the porosity changes when the graphite content change from 8 to 12 wt% at that temperature. Considering the variation observed in the mass loss and the carbon content in the samples after the heat treatments, the hypothesis of soot deposition is reinforced, as well as the fact that more amount of such

kind of carbon was formed in the refractory with higher content of graphite. Taking into account the particular shape of graphite particles and their ability to accommodate in the structure, graphite flakes can be considered as obstacles to pore interconnection, which would contribute reducing the permeability of SB12-0 in respect to SB8-0 after the treatment at 1000 °C, in spite of the higher increase in the apparent porosity, together with the effect of pores blockage by soot deposition. In fact, for the specimens treated at 1000 °C, the permeability was quite similar for SB12-0 (6.1 cm^3/dyn/s) and SB8-0 (6.2 cm^3/dyn/s) [37], as was the proportion of pores <1 μm for both materials (Table 2).

When the refractories were thermally treated at 1400 °C, the same trends discussed for the treatment at 1000 °C were observed. Even when there were higher mass losses at this temperature, especially for SB8-0, the volume of open pores did not show the same degree of increment and SB12-0 exhibited the higher open porosity. In fact, there was a little reduction in the C content in respect to the original amount in the as-received materials, being more pronounced for SB8-0 (~6% compared with a reduction ~1.5% for SB12-0), which manifests the oxidation of this component; due to their characteristics, the soot and the residual carbon were the carbon sources more sensitive to be oxidized. This may be another reason why at this temperature (1400 °C) the proportion of smaller pores (<3 μm) was similar to that of the as-received materials (as the voids occupied by soot were emptied).

It is worth noting that the use of a graphite bed as a way to generate a non-oxidant atmosphere has the advantage of simulating the conditions of the inner part of a MgO–C brick in a vessel lining. When the carbon of the brick's hot face oxidizes, the formed CO may diffuse inside the brick (depending on the chemical potential and thermal gradients). The obtained results suggest that the available CO contributes to the *in situ* formation of additional sources of C as soot, which reduce, block, or close voids in the structure.

3.2. Mechanical properties

The mechanical parameters $E_{0.001}$ (secant elastic modulus), σ_F (fracture strength) and ε_F (fracture strain), together with the value of Δm_M during the thermal exposition in the test, are displayed in Fig. 2.

Regarding the mechanical properties at RT, a tendency of $E_{0.001}$ to decrease with the reduction in the amount of graphite from 12 to 8 wt% is observed (see Fig. 2a), conversely to what was expected considering that graphite is a flexible component (and taking into account that the value of the secant modulus includes elastic as well as non-elastic deformation [41]). This behavior seems to imply that neither Mrozowski cracks [40] nor the flexibility of graphite flakes were determining factors in the deformation during the mechanical loading. In the same direction, the porosity detected in the materials (lower and smaller in SB8-0 than in SB12-0) could not account for the observed differences in the secant-Young modulus values. Thus, the low affinity and interaction between MgO particles and the bonding system could be the reason for the lower rigidity of the SB bricks with 8 wt% graphite [33]. On the other hand, reducing the percentage of graphite increased the mechanical strength of the bricks, as a higher amount of more resistant MgO particles are present, together with a smaller volume of pores (see Fig. 2b). The fracture deformation was also increased when the graphite content varied from 12 to 8 wt%, in spite of the loss of the component with the great ability to deform; this is probably the result of the higher mechanical resistance combined with a lower stiffness exhibited by SB8-0 (see Fig. 2c).

When the evaluation was conducted at high temperatures, the mass losses (Δm_M) showed a similar trend observed with the thermal treatments in graphite bed as a function of graphite content, i.e., higher values for SB8-0 at both temperature levels and the results obtained at 1400 °C duplicate the values at 1000 °C for both compositions (SB12-0 and SB8-0). As the testing temperature was increased, the mechanical

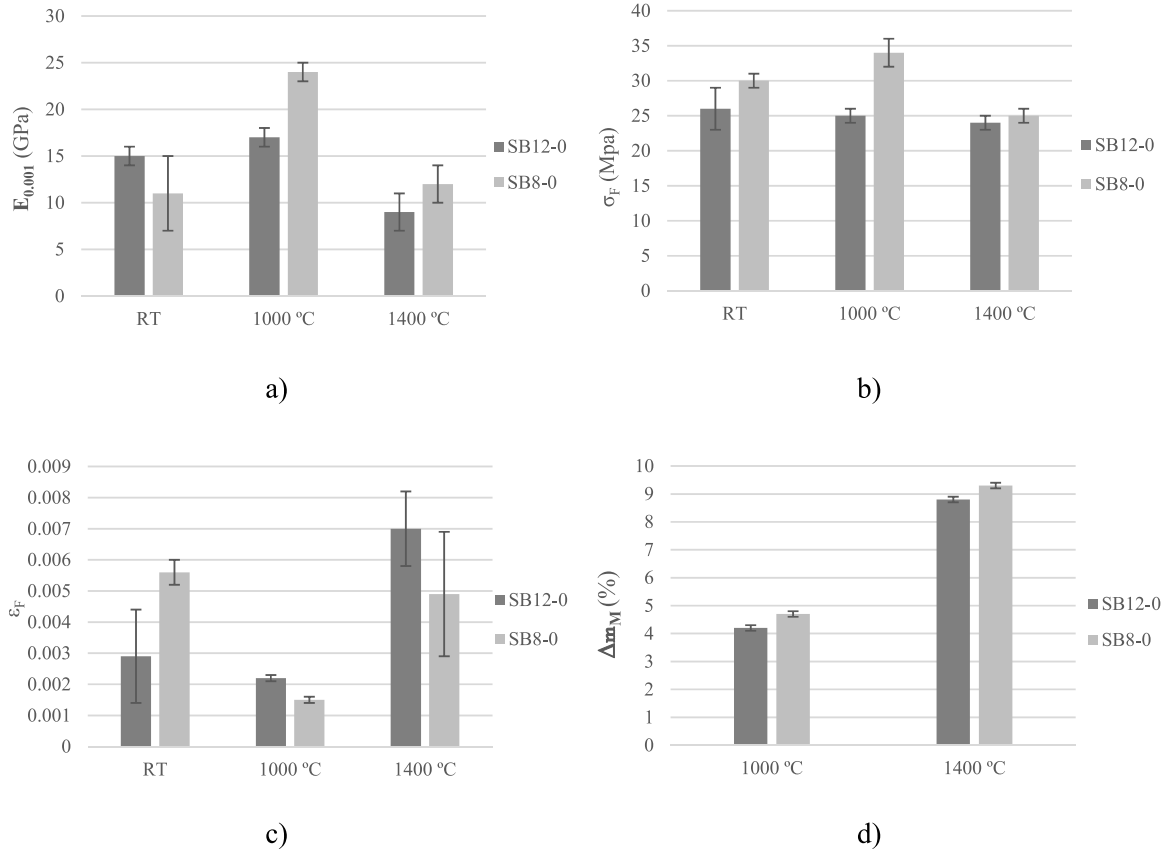

Fig. 2. Mechanical properties at RT, 1000 °C and 1400 °C and values of Δm_M for the mechanical tests at high temperature.

properties varied according to the changes that took place in the refractories and were analyzed in the previous section. The tendency for both materials was the following: when the testing temperature rose up to 1000 °C, the secant modulus and the mechanical strength increased, and the fracture deformation decreased in agreement with these changes, but the opposite was observed when the temperature was further increased up to 1400 °C. The degree of consolidation achieved by the carbonaceous network product of the binder pyrolysis at 1000 °C, was a determining factor working in opposition to other processes which degrade the solid structure, such as increased porosity due to mass loss, opening of channels for gases escape and microcracking. Conversely, these degradation processes, together with the contribution of viscoplasticity, were the dominant factors of the mechanical behavior when the testing temperature was 1400 °C.

However, the changes in the mechanical properties for higher temperatures, although showing a similar tendency for SB12-0 and SB8-0, were more marked for the last material, i.e., the one with lower graphite content. This difference in behavior, between both refractories, for the mechanical properties at high temperatures, would imply that the C–C network development could have a stronger effect than just the porosity changes. For instance, when the specimens were treated at 1000 °C, SB12-0 exhibited a larger change in apparent porosity (more than double between the as-received condition and after 1000 °C treatment, see Tables 1 and 2), although the value of σ_F, for this specimen, was almost unchanged between RT and 1000 °C. It is worth noting that SB8-0 exhibited the highest values of fracture strength and secant modulus, together with the lowest ε_F at 1000 °C. This behavior was also observed by increasing the soaking time at 1000 °C previous to the mechanical loading (from 30 to 60 min) [37]. Considering the evolution of the materials, as it was discussed in the previous section, the distinctive mechanical response of SB8-0 was mainly attributed to: (a) the loss of graphite, which would have more chances to be oxidized as lower amount of the more sensible soot would formed (when compared with SB12-0) and (b) incipient sintering of fine MgO particles, which seem to replace graphite flakes [37], favored by the little pre-load during heating and permanence at high temperature. Unfortunately, from a thermo-mechanical point of view, high mechanical strength and elastic modulus have a negative impact on the thermal shock behavior. Furthermore, less graphite content in MgO–C refractories will affect thermal shock behavior since the flake graphite conductive interface minimizes the thermal stresses; but from another point of view, and seeking alternatives to mitigate this drawback, further research is necessary to evaluate how the deposition of soot impacts this key property.

3.3. Oxidation resistance

The oxidation indicators (decarburized area and Δm_O) of specimens treated in air at 1000 °C and 1400 °C are reported in Fig. 3. The mass loss was divided by the exposed area to obtain comparative values. Moreover, the relative carbon loss was estimated considering that mass reduction was exclusively due to the carbon oxidation (i.e. Δm_O/original carbon content, per area; the original carbon content was determined by the C LECO technique).

From the thermodynamic point of view, the reduction in the amount of graphite leads to a lower oxidation resistance, manifested by a higher carbon loss at temperatures between 1000 °C and 1400 °C, as was reported in a previous work of the authors [42]; moreover, the amount of residual graphite does not change between these temperatures according to the equilibrium calculations [42]. Under the oxidant atmosphere, used for the oxidation test, the pyrolysis of the binder system, as well as the oxidation of the different sources of carbon (residual, soot and

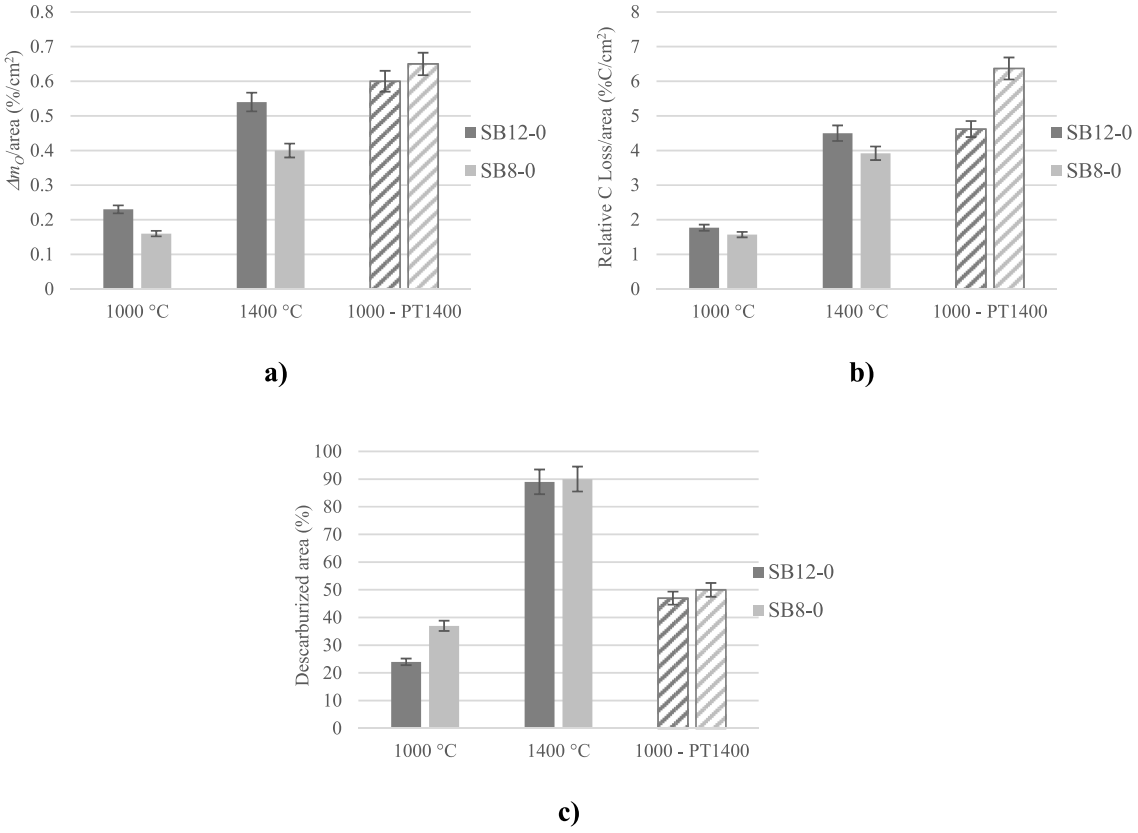

Fig. 3. Oxidation indicators. a) Δm_O per exposed area; b) relative carbon loss per exposed area and c) decarburized area.

graphite), is expected to occur at both testing temperatures. During the previous stages, the specimens were exposed to different thermal treatments (heating and isothermal soaking at 500 °C) which produced several changes in the refractories structures (in the texture and composition), as those previously discussed. These changes, which are dismissed in the equilibrium calculations, as well as other aspects of the systems such as the granulometric ones, partially explain the differences between the thermodynamic predictions and the experimental results, as was already discussed [33,42]. As a consequence of the evolution of such changes, all of the parameters in Fig. 3 indicate that the oxidation resistance of SB12-0 and SB8-0 decrease when the testing temperature rose from 1000 to 1400 °C, as expected.

By considering the decarburized area as an indicator of the oxidation degree, the bricks' resistance at both temperatures (1000 and 1400 °C) lowered as the graphite content was reduced (SB12-0 exhibited smaller decarburized areas, see Fig. 3c). However, if Δm_O and the relative carbon (per unit area) are compared (Fig. 3a and b), the oxidation resistance does not seem to follow the same trend. Conversely, less amount of mass and carbon were lost when the graphite content in the brick's composition decreased, which implies that the oxidation resistance was increased, i.e., SB8-0 > SB12-0.

In other words, higher graphite content in the original composition (SB12-0) involved higher carbon losses with respect to SB8-0. However, this was not translated into an increase in the decarburized area. This particular behavior could be related, on the one hand, to the higher restriction that the reactive gas (O_2) has to enter the interior of SB12-0 (due to the characteristic of its texture, which involved a higher degree of pores blockage, for instance, and probably, its lower permeability after heat-treatment when is compared with SB8-0). On the other hand, it was inferred the presence of a higher amount of soot deposited during the previous thermal treatments in SB12-0, which is a carbonaceous component more susceptible to oxygen attack than graphite. The faster soot oxidation generated a high concentration of gaseous products, whose diffusion toward the outside hindered more effectively the entry of reactive gases into the refractory sample, further reducing the decarburized area. Since the formation of soot can involve the CO coming from the oxidation of the graphite flakes of the bricks, it cannot be discarded that the deposition of soot incorporated additional mass of the sample, increasing the mass loss relative to the initial sample's mass.

An interesting result is obtained when both materials were thermally treated at 1400 °C in graphite bed (1 h), and then, tested at 1000 °C in air (1000-PT1400 in Fig. 3). Under this condition, the three indicators manifest that lower graphite amount in the refractory formulation reduced the oxidation resistance, as shown in Fig. 3 (textured bars). At this point, it is important to consider that the previous thermal history plays an important role to interpret these oxidation results. During the pretreatment at 1400 °C, greater changes in the textural and compositional characteristics of the bricks took place in comparison with those produced during the permanence at 500 °C; at the end of the treatment at 1400 °C, the textures between both bricks were more similar (at least under non-oxidant atmosphere). As was previously mentioned, the experimental data showed that there was a slight oxidation of C even during the treatment at 1400 °C (in graphite bed) in SB8-0, together with the signs of a formation of a lower amount of soot. Considering the complete scenario, it seems that the particular changes, which occurred during the treatment at 500 °C, contribute to mask the lower oxidation resistance in terms of mass/carbon loss when the refractory has lower graphite content in the tested conditions. In other words, the larger mass/carbon loss determined for SB12-0 would let to infer that the material has a lower oxidation resistance; however, probably the more significant amount of mass loss could be attributed to the oxidation of soot (formed during the 500 °C treatment) than the loss of original graphite contained into the as-received product. This could be considered as a strategy to mitigate the effect of the lowering the amount of graphite in the brick's composition on the oxidation resistance. Another important variable to consider is the different carbon-precursors involved in the composition of the MgO–C samples that will lead to different thermal behaviors and produce variations in the type of carbons obtained; thus, this particular outcome will require further studies.

4. Conclusions

In this work, a MgO–C brick with a typical composition for use in the steelmaking industry, with 12 wt% graphite, was evaluated in comparison with a similar material containing just 8 wt% of this component. Aligned with the purpose of reducing the environmental impact, an eco-friendly binder was used in combination with a phenolic resin. The main findings regarding the effect of lowering the graphite content in the brick's composition on the thermal evolution, the mechanical properties, and the oxidation resistance are the following:

- Signs of the formation of soot during thermal treatment at 500 °C and 1000 °C under a non-oxidant atmosphere were found; the amount of such type of carbon seems to be lower for 8 wt% of graphite than for 12 wt% of graphite.
- The mechanical strength was almost constant for the brick with 12 wt% of graphite, whereas the refractory with 8 wt% of graphite exhibited the highest value of this parameter at 1000 °C; the behavior of the latter was explained by the consolidation of the C–C structure produced by the binder pyrolysis, together with an incipient sintering of the finest magnesia particles.
- The decarburized area after treatment at 1000 °C in air was larger for the brick with 8 wt% of graphite, although the mass and carbon losses showed the opposite trend; this particular behavior seems to be a consequence of distinctive changes in the texture and formation of soot during the pre-treatment at 500 °C.

The most interesting results about how the brick performance was affected by the graphite content were those obtained at 1000 °C. This temperature, lower than the maximum operation temperatures, is relevant in any case because some operations are carried out at the intermediate thermal range, as the preheating of ladles, for instance, besides the thermal gradient inside the ladle lining during the campaign implies that the inner part of the brick is around this temperature during long periods of times. The formation of carbon in the bricks during the permanence in the low-middle range of temperatures in the CO atmosphere should be explored as a strategy to mitigate the negative effects of reducing the graphite content.

Declaration of competing interest

The authors declare that they have no known competing financial interests or personal relationships that could have appeared to influence the work reported in this paper.

Acknowledgments

This work was supported by the Agencia Nacional de Promoción Científica y Tecnológica (ANPCyT) of Argentina under projects "Degradación química de refractarios de uso siderúrgico", PICT 2012 N°1215 and "Estudios orientados al tratamiento de problemáticas relacionadas a la fabricación y propiedades en servicio de refractarios óxido-C para la industria del acero" PICT 2017 N°2482. It was also carried out within the scope of the CYTED network 312RT0453 (HOREF). The authors would like to thank Ing. N. Bellandi for providing the refractory bricks.

References

[1] M. Kirschen, K. Badr, J. Cappel, A. Drescher, A cost-effective method to reduce energy consumption and CO2 emissions in steelmaking, Stahl Eisen 129 (2009).

[2] M. Kirschen, A. Drescher, K. Badr, J. Cappel, Intelligent refractory systems: a cost-effective method to reduce energy consumption and CO2 emissions in steelmaking, RHI Bull 2 (2010) 43–48. https://www.researchgate.net/publication/276408007.

[3] S. Biswas, D. Sarkar, Introduction to Refractories for Iron- and Steelmaking, 2020, https://doi.org/10.1007/978-3-030-43807-4.

[4] V. Colla, T.A. Branca, R. Pietruck, S. Wölfelschneider, A. Morillon, D. Algermissen, S. Rosendahl, H. Granbom, U. Martini, D. Snaet, Future research and developments on reuse and recycling of steelmaking by-products, Metals (Basel) 13 (2023) 1–26, https://doi.org/10.3390/met13040676.

[5] T. Zhu, Y. Li, S. Sang, Z. Xie, Mechanical behavior and thermal shock resistance of MgO-C refractories: influence of graphite content, Ceram. Int. 43 (2017) 7177–7183, https://doi.org/10.1016/j.ceramint.2017.03.004.

[6] X. Xu, Y. Li, Y. Dai, T. Zhu, L. Pan, J. Szczerba, Influence of graphite content on fracture behavior of MgO–C refractories based on wedge splitting test with digital image correlation method and acoustic emission, Ceram. Int. 47 (2021) 12742–12752, https://doi.org/10.1016/j.ceramint.2021.01.134.

[7] Y. Liu, Q. Wang, G. Li, J. Zhang, W. Yan, A. Huang, Role of graphite on the corrosion resistance improvement of MgO–C bricks to MnO-rich slag, Ceram. Int. 46 (2020) 7517–7522, https://doi.org/10.1016/j.ceramint.2019.11.250.

[8] Z. Liu, J. Yu, S. Yue, D. Jia, E. Jin, B. Ma, L. Yuan, Effect of carbon content on the oxidation resistance and kinetics of MgO-C refractory with the addition of Al powder, Ceram. Int. 46 (2020) 3091–3098, https://doi.org/10.1016/j.ceramint.2019.10.010.

[9] M. Bag, S. Adak, R. Sarkar, Nano carbon containing MgO-C refractory: effect of graphite content, Ceram. Int. 38 (2012) 4909–4914, https://doi.org/10.1016/j.ceramint.2012.02.082.

[10] S. Mahato, S.K. Pratihar, S.K. Behera, Fabrication and properties of MgO-C refractories improved with expanded graphite, Ceram. Int. 40 (2014) 16535–16542, https://doi.org/10.1016/j.ceramint.2014.08.007.

[11] K.S. Lee, G.H. Jo, Y.G. Jung, Y. Byeun, Effect of carbon content on the mechanical behavior of MgO-C refractories characterized by Hertzian indentation, Ceram. Int. 42 (2016) 9955–9962, https://doi.org/10.1016/j.ceramint.2016.03.097.

[12] T. Zhu, Y. Li, S. Sang, Z. Xie, A new approach to fabricate MgO-C refractories with high thermal shock resistance by adding artificial graphite, J. Eur. Ceram. Soc. 38 (2018) 2179–2185, https://doi.org/10.1016/j.jeurceramsoc.2017.10.018.

[13] Y. Cheng, T. Zhu, Y. Li, S. Sang, Microstructure and properties of MgO–C refractory with different carbon contents, Ceram. Int. 47 (2021) 2538–2546, https://doi.org/10.1016/j.ceramint.2020.09.099.

[14] M. Bag, S. Adak, R. Sarkar, Study on low carbon containing MgO-C refractory: use of nano carbon, Ceram. Int. 38 (2012) 2339–2346, https://doi.org/10.1016/j.ceramint.2011.10.086.

[15] T. Zhu, Y. Li, M. Luo, S. Sang, Q. Wang, L. Zhao, Y. Li, S. Li, Microstructure and mechanical properties of MgOC refractories containing graphite oxide nanosheets (GONs), Ceram. Int. 39 (2013) 3017–3025, https://doi.org/10.1016/j.ceramint.2012.09.080.

[16] J. Chen, Y. Du, Y. Zhang, M. Nath, W. Yan, Y. Wei, S. Zhang, N. Li, Oxidation behaviors of low carbon MgO-C refractories: roles of Ti 2 AlC and Ti 2 AlN, J. Am. Ceram. Soc. (2023) 4411–4424, https://doi.org/10.1111/jace.19100.

[17] X. Wang, C. Deng, J. Di, G. Xing, J. Ding, H. Zhu, C. Yu, Enhanced oxidation resistance of low-carbon MgO–C refractories with Al3BC3–Al antioxidants: a synergistic effect, J. Am. Ceram. Soc. 106 (2023) 3749–3764, https://doi.org/10.1111/jace.19023.

[18] T. Zhu, Y. Li, S. Sang, S. Jin, Y. Li, L. Zhao, X. Liang, Effect of nanocarbon sources on microstructure and mechanical properties of MgO-C refractories, Ceram. Int. 40 (2014) 4333–4340, https://doi.org/10.1016/j.ceramint.2013.08.101.

[19] G. Wei, B. Zhu, X. Li, Z. Ma, Microstructure and mechanical properties of low-carbon MgO-C refractories bonded by an Fe nanosheet-modified phenol resin, Ceram. Int. 41 (2015) 1553–1566, https://doi.org/10.1016/j.ceramint.2014.09.091.

[20] A.V. Maldhure, A.V. Wankhade, In-situ development of carbon nanotubes network and graphitic carbon by catalytic modification of phenolic resin binder in Al 2 O 3 –MgO–C refractories, J. Asian Ceram. Soc. 5 (2017) 247–254, https://doi.org/10.1016/j.jascer.2017.04.010.

[21] T. Zhu, Y. Li, S. Sang, Z. Xie, Improved thermal shock resistance of magnesia-graphite refractories by the addition of MgO-C pellets, Mater. Des. 124 (2017) 16–23, https://doi.org/10.1016/j.matdes.2017.03.054.

[22] T. Zhu, Y. Li, S. Sang, Z. Xie, Fracture behavior of low carbon MgO–C refractories using the wedge splitting test, J. Eur. Ceram. Soc. 37 (2017) 1789–1797, https://doi.org/10.1016/j.jeurceramsoc.2016.11.013.

[23] Y. Yang, J. Yu, H. Zhao, H. Zhang, P. Zhao, Y. Li, X. Wang, G. Li, Cr7C3: a potential antioxidant for low carbon MgO–C refractories, Ceram. Int. 46 (2020) 19743–19751, https://doi.org/10.1016/j.ceramint.2020.04.298.

[24] Y. Chen, J. Ding, C. Yu, X. Lou, Z. Wu, C. Deng, Application of SiC whiskers synthesized from waste rice husk in low-carbon MgO–C refractories, J. Phys. Chem. Solid. 177 (2023), 111304, https://doi.org/10.1016/j.jpcs.2023.111304.

[25] Y. Chen, J. Ding, C. Deng, C. Yu, Improved thermal shock stability and oxidation resistance of low-carbon MgO– C refractories with introduction of SiC whiskers Yang, Ceram. Int. (2023), 111228, https://doi.org/10.1016/j.ceramint.2023.05.224.

[26] S. Nanda, A. Choudhury, K.S. Chandra, D. Sarkar, Raw materials, microstructure, and properties of MgO–C refractories: directions for refractory recipe development, J. Eur. Ceram. Soc. 43 (2023) 14–36, https://doi.org/10.1016/j.jeurceramsoc.2022.09.032.

[27] C.G. Aneziris, J. Hubálková, R. Barabás, Microstructure evaluation of MgO-C refractories with TiO2- and Al-additions, J. Eur. Ceram. Soc. 27 (2007) 73–78, https://doi.org/10.1016/j.jeurceramsoc.2006.03.001.

[28] A.P. Luz, C.G. Renda, A.A. Lucas, R. Bertholdo, C.G. Aneziris, V.C. Pandolfelli, Graphitization of phenolic resins for carbon-based refractories, Ceram. Int. 43 (2017) 8171–8182, https://doi.org/10.1016/j.ceramint.2017.03.143.

[29] S.I. Talabi, A.P. Luz, A.A. Lucas, C. Pagliosa, V.C. Pandolfelli, Catalytic graphitization of novolac resin for refractory applications, Ceram. Int. 44 (2018) 3816–3824, https://doi.org/10.1016/j.ceramint.2017.11.167.

[30] A.P. Luz, R. Salomão, C.S. Bitencourt, C.G. Renda, A.A. Lucas, C.G. Aneziris, V. C. Pandolfelli, Thermosetting resins for carbon-containing refractories: theoretical basis and novel insights, Open Ceram 3 (2020), 100025, https://doi.org/10.1016/j.oceram.2020.100025.

[31] Z. Yang, B. Liu, H. Zhao, J. Li, X. Guo, D. Zhang, Z. Liu, Pyrolysis mechanism of composite binder composed of coal tar pitch and phenolic resin for carbon materials, J. Anal. Appl. Pyrolysis 169 (2023), 105840, https://doi.org/10.1016/j.jaap.2022.105840.

[32] C.L. Pássera, L.B. Manfredi, A.G. Tomba Martinez, Study of the thermal behavior of organic binders used in oxide-carbon refractory bricks, Metall. Mater. Trans. B 52 (2021) 1681–1694.

[33] M.N. Moliné, S.E. Gass, P.G. Galliano, A.G. Tomba Martinez, The effects of binder type combined with graphite content and the presence of aluminum on the characteristics of MgO–C bricks, Ceram. Int. 48 (2022) 34627–34634, https://doi.org/10.1016/j.ceramint.2022.08.050.

[34] N. Nishiyama, T. Yokoyama, Permeability of porous media: role of the critical pore size, J. Geophys. Res. Solid Earth 122 (2017) 6955–6971, https://doi.org/10.1002/2016JB013793.

[35] DIN EN 993-1, DIN 51056 - Method of Test for Dense Shaped Refractory Products. Determination of Bulk Density, Apparent Porosity and True Porosity, 1995.

[36] V. Muñoz, G.A. Rohr, A.L. Cavalieri, A.G. Tomba Martinez, Experimental procedure for the mechanical evaluation of oxide-carbon refractories by strain measurement, J. Test. Eval. 40 (2012), https://doi.org/10.1520/jte103455.

[37] S.E. Gass, P.G. Galliano, A.G. Tomba Martinez, Impact of preheating on the mechanical performance of different MgO-C bricks—intermediate temperature range, J. Eur. Ceram. Soc. 41 (2021) 3769–3781, https://doi.org/10.1016/j.jeurceramsoc.2021.01.025.

[38] S.K. Sadrnezhaad, S. Mahshid, B. Hashemi, Z.A. Nemati, Oxidation mechanism of C in MgO-C refractory bricks, J. Am. Ceram. Soc. 89 (2006) 1308–1316, https://doi.org/10.1111/j.1551-2916.2005.00863.x.

[39] X. Li, M. Rigaud, Anisotropy uf the properties of magnesia-graphite refractories, J. Can. Ceram. Soc. 62 (1993) 197–205.

[40] C. Baudin, High temperature mechanical behavior of magnesia-graphite refractories Carmen, Am. Ceram. Soc. 125 (2001) 73–92.

[41] V. Muñoz, A.G.T. Martinez, Factors controlling the mechanical behavior of alumina-magnesia-carbon refractories in air, Ceram. Int. 42 (2016) 11150–11160, https://doi.org/10.1016/j.ceramint.2016.04.021.

[42] S.E. Gass, W.A. Calvo, M.N. Moliné, P.G. Galliano, A.G.T. Martinez, Combined effects of the graphite content and addition of aluminum in the characteristics of resin-bonded MgO-C bricks, Mater. Today Commun. 30 (2022), https://doi.org/10.1016/j.mtcomm.2021.103057.